Suppressing decoherence of spin waves in a warm atomic vapor by applying a guiding magnetic field

2015 J. Phys. B: At. Mol. Opt. Phys. 48 035506

(http://iopscience.iop.org/0953-4075/48/3/035506)

IOP Publishing Journal of Physics B: Atomic, Molecular and Optical Physics
J. Phys. B: At. Mol. Opt. Phys. **48** (2015) 035506 (11pp) doi:10.1088/0953-4075/48/3/035506

Suppressing decoherence of spin waves in a warm atomic vapor by applying a guiding magnetic field

Long Tian, Shujing Li, Zhiying Zhang and Hai Wang

The State Key Laboratory of Quantum Optics and Quantum Optics Devices, Institute of Opto-Electronics, Shanxi University, Taiyuan, 030006, People's Republic of China

E-mail: wanghai@sxu.edu.cn

Received 10 September 2014, revised 5 November 2014
Accepted for publication 24 November 2014
Published 13 January 2015

Abstract

We report an experimental and theoretical investigation to extend lifetimes of light storages by applying guiding magnetic fields in a room-temperature atomic vapor. The storages are based on dynamic electromagnetically induced transparency. Retrieval efficiencies versus storage time are experimentally measured for different strengths of the guiding magnetic fields. The measured results show that the $1/e$ storage times are $\sim 6\,\mu$s and $\sim 59\,\mu$s for the guiding field $B_{0z} = 0$ and $B_{0z} = 93$ mG, respectively. Physical processes causing decoherence in an atomic ensemble have been discussed and analyzed. A theory model which is used to evaluate the decoherence caused by fluctuations of transverse magnetic fields is developed. Based on this evaluation, the fact that storage lifetimes can be increased by applying guiding magnetic fields is well explained.

Keywords: suppressing decoherence of spin waves, light storages, electromagnetically induced transparency, guiding magnetic fields, room-temperature atomic vapor

(Some figures may appear in colour only in the online journal)

1. Introduction

The optical storage is an important step toward the realization of long-distance quantum communications and quantum information processing [1–4]. To implement this task, key performance benchmarks of light storage such as long lifetimes, high efficiencies are required. Over the past decade, a variety of physical processes, such as electromagnetically induced transparency (EIT) [5], spontaneous Raman emission [3], gradient echo [6], far-off-resonant Raman interaction [7] and others [8–11] have been developed into promised storage schemes. Optical storages based on these schemes have been realized in various media such as cold atomic gases [12–14], room-temperature atomic vapors [8, 15–26] and cryogenically-cooled solid devices [9]. For the practical use of quantum memories, their experimental complexity has to be reduced. The room-temperature (warm) atomic vapor is a simple and robust storage medium since its operation does not need laser trapping and high vacuum or cryogenic cooling. In room-temperature atomic vapors, EIT-based storages of classical light pulses [15–18] and of optical quantum states [19–26] have been successfully implemented. For suppressing ground-state decoherence, vapor cells are filled with buffer gas (or cell walls are paraffin-coated) and placed in magnetically shields in these experiments. The storage lifetimes in most of the experiments are not more than 10 μs [16–26], the longest lifetime achieved in the off-resonant Faraday interaction scheme [8] was up to $\sim$1 ms. Recently, the experiments that the lifetimes of qubit memories are significantly increased by applying weak guide magnetic fields have been demonstrated in trapped single-atom system [27]. Such increases in lifetimes are attributed to that the guiding fields suppress the influences of transverse magnetically fluctuations on the absolute field stability [27, 28]. However, there is not a theoretical model to well explain this effect until now. Also, the increase in lifetime by applying a guiding magnetic field has not been studied in light storages based on room-temperature atomic vapors.

In this paper, we report an experimental and theoretical investigation to extend the lifetimes of light storages by

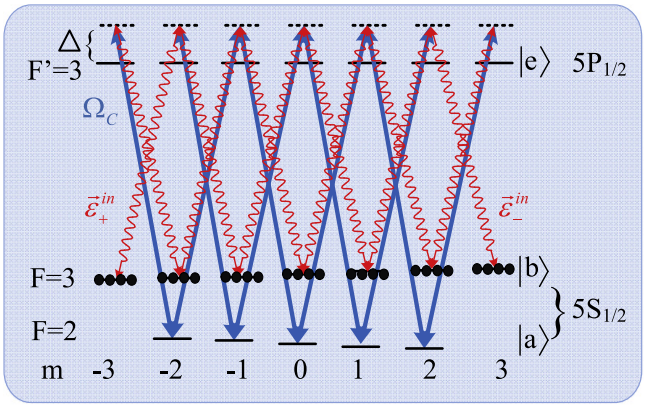

Figure 1. The involved levels of ^{85}Rb atoms. $\vec{\varepsilon}_{+}^{\,\mathrm{in}}$ and $\vec{\varepsilon}_{-}^{\,\mathrm{in}}$ are the right- and left-circularly-polarized signal fields, respectively. Ω_{C} denotes the controlling field.

applying guiding magnetic fields in a room-temperature atomic vapor. The storages are based on dynamic EIT. Retrieval efficiencies are measured for different strengths of the guiding magnetic fields. When no guiding magnetic field is applied, the $1/e$ storage time is $\sim 6\,\mu$s. While, when a weak guiding magnetic field (~ 93 mG) is applied, the $1/e$ storage time becomes $\sim 59\,\mu$s. We developed a theory to model the decoherence process caused by fluctuations of transverse magnetic fields. Based on this model, the reason that the storage time can be increased by applying a large enough guiding magnetic field is well explained.

This paper is organized as follows. In section 2, we discuss the theory of the EIT-based light storages in multiple Λ-systems. In section 3, we describe experimental setup, implementation and results for the light storages. In section 4, we discuss the reasons for suppressing decoherence of spin waves by applying a guiding magnetic field. Finally, a brief conclusion is given in section 5.

2. EIT-based light storage in multiple Λ-systems

The involved levels of ^{85}Rb atoms are shown in figure 1, where $|a\rangle = |5S_{1/2}, F = 2\rangle$, $|b\rangle = |5S_{1/2}, F = 3\rangle$, $|e\rangle = |5P_{1/2}, F' = 3\rangle$. The strong vertical-linearly- (V-) polarized controlling light field and the weak horizontal-linearly- (H-) polarized signal light field are respectively tuned to the transitions $|a\rangle \leftrightarrow |e\rangle$ and $|b\rangle \leftrightarrow |e\rangle$ with a blue detuning Δ. The quantum axis is defined along the z-direction, which is the same as the propagating directions of the two light beams. In this case, the H-polarized signal light field can be divided into the right (helicity $\alpha = 1$) and left ($\alpha = -1$) circular polarization components, which drive $|b, m_b\rangle \leftrightarrow |e, m_e = m_b + 1\rangle$ and $|b, m_b\rangle \leftrightarrow |e, m_e = m_b - 1\rangle$ transitions, respectively, and the V-polarized controlling light field also is divided into the right and left circular components, which drive $|a, m_a\rangle \leftrightarrow |e, m_e = m_a + 1\rangle$ and $|a, m_a\rangle \leftrightarrow |e, m_e = m_a - 1\rangle$ transitions, respectively. The H-polarized signal field can be represented as

$$\vec{\varepsilon}_{H}^{\,\mathrm{in}}(z,t) = \frac{\vec{\varepsilon}_{+}^{\,\mathrm{in}}(z,t) + \vec{\varepsilon}_{-}^{\,\mathrm{in}}(z,t)}{\sqrt{2}}, \tag{1}$$

where, $\vec{\varepsilon}_{+}^{\,\mathrm{in}}(z,t) = \varepsilon_{H}^{\mathrm{in}}(z,t)\vec{e}_{+}$ and $\vec{\varepsilon}_{-}^{\,\mathrm{in}}(z,t) = \varepsilon_{H}^{\mathrm{in}}(z,t)\vec{e}_{-}$ are the right-circularly-polarized and left-circularly-polarized signal fields, respectively, $\vec{e}_{+} = \frac{1}{\sqrt{2}}\begin{pmatrix}1\\-\mathrm{i}\end{pmatrix}$ and $\vec{e}_{-} = \frac{1}{\sqrt{2}}\begin{pmatrix}1\\\mathrm{i}\end{pmatrix}$ are the two unit vectors in the H/V basis, $\varepsilon_{H}^{\mathrm{in}}(z,t) = \left|\vec{\varepsilon}_{H}^{\,\mathrm{in}}(z,t)\right|$ is the amplitude of the signal field. Due to optical pumping by the strong controlling light, most of the atoms will be prepared in every Zeeman sublevel $|b, m_b\rangle$ with an equal probability $p = 1/(2F_b + 1)$. In this case, multiple Λ-type EIT configurations are formed (figure 1). The storage and retrieval processes for the signal fields $\vec{\varepsilon}_{+}^{\,\mathrm{in}}(z,t)$ and $\vec{\varepsilon}_{-}^{\,\mathrm{in}}(z,t)$ can be described by the dark-state polariton concepts [5, 29, 30]

$$\hat{\Psi}_{\pm}(z,t) = \cos\vartheta\vec{\varepsilon}_{\pm}^{\,\mathrm{in}}(z,t) - \sin\vartheta\sqrt{Np}\,\hat{S}_{\pm}(z,t), \tag{2}$$

where, $\cos\vartheta(t) = \Omega_{\mathrm{C}}(t)/\sqrt{g^2Np + |\Omega_{\mathrm{C}}(t)|^2}$, $\sin\vartheta(t) = g\sqrt{Np}/\sqrt{g^2Np + |\Omega_{\mathrm{C}}(t)|^2}$, $\Omega_{\mathrm{C}}(t)$ is the Rabi frequency of the controlling field, N is total number of atoms, g is the atom-field coupling constant, $\hat{S}_{\pm}(z,t)$ are the spin waves which are created by mapping $\vec{\varepsilon}_{\pm}^{\,\mathrm{in}}(z,t)$ fields into the atomic ensembles and can be expressed as [31, 32]:

$$\hat{S}_{+}(z,t) = \frac{\sum_{m_a=-2}^{2} R_{m_a,\alpha=1}^{\beta=\alpha}\rho_{m_a,m_b=m_a}^{(+)}(z,t) + \sum_{m_a=-1}^{2} R_{m_a,\alpha=1}^{\beta=-\alpha}\rho_{m_a,m_b=m_a-2}^{(+)}(z,t)}{\sqrt{\left(\sum_{m_a=-2}^{2}\left|R_{m_a,\alpha=1}^{\beta=\alpha}\right|^2 + \sum_{m_a=-1}^{2}\left|R_{m_a,\alpha=1}^{\beta=-\alpha}\right|^2\right)}}, \tag{3a}$$

$$\hat{S}_{-}(z,t) = \frac{\sum_{m_a=-2}^{2} R_{m_a,\alpha=-1}^{\beta=\alpha}\rho_{m_a,m_b=m_a}^{(-)}(z,t) + \sum_{m_a=-2}^{1} R_{m_a,\alpha=-1}^{\beta=-\alpha}\rho_{m_a,m_b=m_a+2}^{(-)}(z,t)}{\sqrt{\left(\sum_{m_a=-2}^{2}\left|R_{m_a,\alpha=-1}^{\beta=\alpha}\right|^2 + \sum_{m_a=-2}^{1}\left|R_{m_a,\alpha=-1}^{\beta=-\alpha}\right|^2\right)}}, \tag{3b}$$

respectively, where $\rho_{m_a,m_b}^{(\pm)}(z,t) = N_z^{-1}\sum_{z_j\in N_z}|a, m_a\rangle\langle b, m_b|\,\mathrm{e}^{-\mathrm{i}\omega_{m_a,m_b}t}$ is the spin-wave operator associated with the coherence between the Zeeman sublevels $|a, m_a\rangle$ and $|b, m_b\rangle$, superscripts $\pm$ correspond to Zeeman coherences generated by storing the signal fields $\vec{\varepsilon}_{+}^{\,in}(z,t)$ and $\vec{\varepsilon}_{-}^{\,in}(z,t)$, respectively, $N_z = N\mathrm{d}z/l$ is the number of atoms between z and $z+\mathrm{d}z$, l is the length of the vapor cell, $\omega_{m_a,m_b} = \omega_{m_a,m_b}^{0} + \omega_{m_a,m_b}^{Bz}$, ω_{m_a,m_b}^{0} is the frequency splitting between the hyperfine states

$\left|5S_{1/2}, F=2\right\rangle$ and $\left|5S_{1/2}, F=3\right\rangle$, $\omega^{Bz}_{m_a,m_b}$ is the Zeeman frequency shift of the transition $\left|a, m_a\right\rangle \leftrightarrow \left|b, m_b\right\rangle$, which can be expressed as:

$$\omega^{B_z}_{m_a,m_b} = \frac{\mu_B B_z}{\hbar}\left(g_{F_a}(m_a+m_b) - \delta g m_b\right), \tag{4}$$

here, B_z is the magnetic field along z axis, $\delta g = g_{F_a} + g_{F_b} \approx -0.00011$, $g_{F_a} \approx -0.33417$, $g_{F_b} \approx 0.33406$ are the Landé factors for $|a\rangle$ and $|b\rangle$ states, respectively. The factors $R^{\beta=\alpha}_{m_a,\alpha} = C^{F_b 1 F_e}_{m_a\alpha(m_a+\alpha)}/C^{F_a 1 F_e}_{m_a\beta(m_a+\alpha)}$, $R^{\beta=-\alpha}_{m_a,\alpha} = C^{F_b 1 F_e}_{(m_a-\alpha+\beta)\alpha(m_a+\beta)}/C^{F_a 1 F_e}_{m_a\beta(m_a+\beta)}$ [31, 32] describe the contributions of the coherences $\rho_{m_a,m_b}(z,t)$ to the spin waves $S_{\pm}(z,t)$, where, $C^{F_b 1 F_e}_{m_b\beta(m_b+\beta)}$ and $C^{F_a 1 F_e}_{m_a\alpha(m_a+\alpha)}$ are the Clebsch–Gordon coefficients for the transitions $|b\rangle \leftrightarrow |e\rangle$ and $|a\rangle \leftrightarrow |e\rangle$. According to the definitions of $R^{\beta=\pm\alpha}_{m_a,\alpha}$, we have:

$$\sum_{m_a=-2}^{2}\left|R^{\beta=\alpha}_{m_a,\alpha=1}\right|^2 + \sum_{m_a=-1}^{2}\left|R^{\beta=-\alpha}_{m_a,\alpha=1}\right|^2 = \sum_{m_a=-2}^{2}\left|R^{\beta=\alpha}_{m_a,\alpha=-1}\right|^2 + \sum_{m_a=-2}^{1}\left|R^{\beta=-\alpha}_{m_a,\alpha=-1}\right|^2 = |R|^2. \tag{5}$$

According to the dark-state polariton concepts in equation (2), we see that the signal fields $\hat{\varepsilon}^{in}_{\pm}(z,t)$ can be mapped onto $\hat{S}_{\pm}(z,t)$, respectively, when the controlling beams $\left(\Omega_C\right)$ are adiabatically turned off over a very short time interval $[t_{0-}, t_0]$ (in the presented experiment, the time interval is $\delta t = t_0 - t_{0-} \approx 50$ ns). The initially stored Zeeman coherences $\rho^{(\pm)}_{m_a,m_b}(z,t_0)$ can be written as:

$$\rho^{(+)}_{m_a,m_b=m_a}(z,t_0) \propto \frac{R^{\beta=\alpha}_{m_a,\alpha=1}}{\sqrt{2R^2}}\varepsilon^{\rm in}_H(z-z_{01},t_{0-}), \tag{6a}$$

$$\rho^{(+)}_{m_a,m_b=m_a-2}(z,t_0) \propto \frac{R^{\beta=-\alpha}_{m_a,\alpha=1}}{\sqrt{2R^2}}\varepsilon^{\rm in}_H(z-z_{01},t_{0-}), \tag{6b}$$

$$\rho^{(-)}_{m_a,m_b=m_a}(z,t_0) \propto \frac{R^{\beta=\alpha}_{m_a,\alpha=-1}}{\sqrt{2R^2}}\varepsilon^{\rm in}_H(z-z_{01},t_{0-}), \tag{6c}$$

$$\rho^{(-)}_{m_a,m_b=m_a+2}(z,t_0) \propto \frac{R^{\beta=-\alpha}_{m_a,\alpha=-1}}{\sqrt{2R^2}}\varepsilon^{\rm in}_H(z-z_{01},t_{0-}), \tag{6d}$$

where $z_{01} = \int_{t_{0-}}^{t_0} {\rm d}t' v_g(t')$, $v_g(t)$ is the group speed of signal pulse. Each Zeeman coherences $\rho_{m_a,m_b}(z,t)$ will suffer from decoherence and experience Larmor precessions during the storage time interval of t and will evolve into:

$$\rho_{m_a,m_b}(z,t) = \rho_{m_a,m_b}(z,t_0){\rm e}^{-f_{m_a,m_b}(t-t_0)}{\rm e}^{-{\rm i}\omega_{m_a,m_b}(t-t_0)} \simeq \rho_{m_a,m_b}(z,t_0){\rm e}^{-f_{m_a,m_b}(t)}{\rm e}^{-{\rm i}\omega_{m_a,m_b}t}, \tag{7}$$

where, $t_0 = 0$ is assumed, $f_{m_a,m_b}(t)$ is the decoherence factor of the spin wave $\rho_{m_a,m_b}(z,t)$, which will be given in section 4. By switching on the reading light, the stored spin waves $S_{\pm}(t)$ will be transferred into right-and left-circularly-polarized retrieved light fields respectively. The retrieval efficiency mainly depends on the optical depth [30, 33]. Since the prepared atoms in Zeeman sublevel $\left|b, m_b\right\rangle$ are unpolarized, the absorption coefficients of $\sigma^{\pm}$-circularly-polarized components of the signal light are the same. Thus, the retrieval efficiencies of $\sigma^{\pm}$-components are the same, which means that the retrieved field amplitudes of $\sigma^{\pm}$-components are equal. So, the retrieved signal field amplitudes can be written as:

$$\vec{\varepsilon}^{\,\rm out}_{+}(z,t) \propto \frac{\varepsilon^{\rm in}_H(z-z_{01},t_{0-})}{\sqrt{2}R^2}{\rm e}^{-{\rm i}\omega^0_{m_a,m_b}t} \times\left(\sum_{m_a=-2}^{2}\left|R^{\beta=\alpha}_{m_a,\alpha=1}\right|^2{\rm e}^{-f_{m_a,m_b}(t)}{\rm e}^{-{\rm i}\omega^{B_z}_{m_a,m_b}t} + \sum_{m_a=-1}^{2}\left|R^{\beta=-\alpha}_{m_a,\alpha=1}\right|^2{\rm e}^{-f_{m_a,m_b}(t)}{\rm e}^{-{\rm i}\omega^{B_z}_{m_a,m_b}t}\right), \tag{8a}$$

$$\vec{\varepsilon}^{\,\rm out}_{-}(z,t) \propto \frac{\varepsilon^{\rm in}_H(z-z_{01},t_{0-})}{\sqrt{2}R^2}{\rm e}^{-{\rm i}\omega^0_{m_a,m_b}t} \times\left(\sum_{m_a=-2}^{2}\left|R^{\beta=\alpha}_{m_a,\alpha=-1}\right|^2{\rm e}^{-f_{m_a,m_b}(t)}{\rm e}^{-{\rm i}\omega^{B_z}_{m_a,m_b}t} + \sum_{m_a=-2}^{1}\left|R^{\beta=-\alpha}_{m_a,\alpha=-1}\right|^2{\rm e}^{-f_{m_a,m_b}(t)}{\rm e}^{-{\rm i}\omega^{B_z}_{m_a,m_b}t}\right). \tag{8b}$$

The retrieved H-polarized field is

$$\vec{\varepsilon}^{\,\rm out}_{H}(z,t) = \frac{\vec{\varepsilon}^{\,\rm out}_{+}(z,t) + \vec{\varepsilon}^{\,\rm out}_{-}(z,t)}{\sqrt{2}}. \tag{9}$$

The definition of time-dependence retrieval efficiency $\eta_H(t)$ is $\eta_H(t) = \int\left|\vec{\varepsilon}^{\,\rm out}_H(t,z)\right|^2{\rm d}z / \int\left|\vec{\varepsilon}^{\,\rm in}_H(t_{0-},z)\right|^2{\rm d}z$, where $\int\left|\vec{\varepsilon}^{\,\rm in}_H(t_{0-},z)\right|^2{\rm d}z$ corresponds to the numbers of the incoming signal photons and $\int\left|\vec{\varepsilon}^{\,\rm out}_H(t,z)\right|^2{\rm d}z$ corresponds to the photon numbers retrieved from the spin wave at the storage time t. According to this definition together with equations (8) and (9), we obtain:

$$\eta_H(t) = \eta_H(0)\left|\frac{1}{2R^2}\left[\sum_{m_a=-2}^{2}\left|R^{\beta=\alpha}_{m_a,\alpha=1}\right|^2{\rm e}^{-f_{m_a,m_b}(t)-{\rm i}\omega^{B_z}_{m_a,m_b}t} + \sum_{m_a=-1}^{2}\left|R^{\beta=-\alpha}_{m_a,\alpha=1}\right|^2{\rm e}^{-f_{m_a,m_b}(t)-{\rm i}\omega^{B_z}_{m_a,m_b}t} + \sum_{m_a=-2}^{2}\left|R^{\beta=\alpha}_{m_a,\alpha=-1}\right|^2{\rm e}^{-f_{m_a,m_b}(t)-{\rm i}\omega^{B_z}_{m_a,m_b}t} + \sum_{m_a=-2}^{1}\left|R^{\beta=-\alpha}_{m_a,\alpha=-1}\right|^2{\rm e}^{-f_{m_a,m_b}(t)-{\rm i}\omega^{B_z}_{m_a,m_b}t}\right]\right|^2, \tag{10}$$

where, $\eta_H(0)$ is the retrieval efficiency at initial time $t = t_0 = 0$.

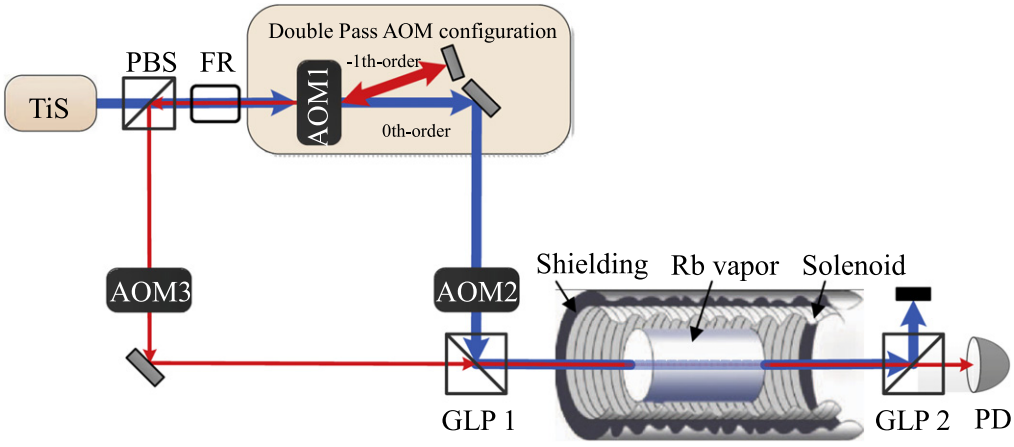

Figure 2. Experimental set-up. PBS: polarization beam splitter; AOM1: 1.7 GHz acousto-optic modulator; AOM2–3: 200 MHz acousto-optic modulators; FR: Faraday rotator; GLP1–2: Glan-laser polarizers; PD: Photodetector.

3. Experimental setup, implementation and results of EIT-based light storages

The experimental setup is schematically shown in figure 2. A Ti:Sapphire (MBR-110) laser beam goes through a polarization beam splitter (PBS) and then is sent to a acousto-optic modulator (AOM1) with a fast modulation frequency of 1.717 87 GHz. The zeroth-order output of the laser from AOM1 is used as the controlling beam. The first-order output of the laser from AOM1 is retroreflected for a second pass through AOM1. The first-order output of the second pass counter-propagates with the original input laser beam, it serves as the signal light beam. After going through the AOM1 in the double-pass configuration, the frequency of the signal beam is shift down by 3.435 GHz. The signal beam is rotated by 90° with a Faraday rotator and then reflected by the PBS. The signal and controlling beams are sent through two acousto-optic modulators (AOM3 and AOM2) for switching on/off them, respectively. AOM2 and AOM3 are driven by one signal source operating at a radio-frequency of $\mp$200 MHz, respectively. So, after AOM2 and AOM3 the frequency difference between the signal and controlling light beams becomes 3.035 GHz, which is equal to the hyperfine splitting between two ground levels of ^{85}Rb. The detuning of the controlling (signal) beam is $\Delta \approx 1.4$ GHz to the blue of the transition $\left|5S_{1/2}, F=2\right\rangle \leftrightarrow \left|5P_{/2}, F'=3\right\rangle$ $\left(\left|5S_{1/2}, F=3\right\rangle \leftrightarrow \left|5P_{/2}, F'=3\right\rangle\right)$. A Glan laser polarizer (GLP1) is used to combine the H-polarized signal beam and V-polarized controlling beams. The combined beams goes thought quartz cell along z axis. The cell is filled with pure ^{85}Rb vapor as well as 10 Torr Ne buffer gas and heated to ~53 °C. Its length and diameter are $l=75$ mm and $d=25$ mm, respectively. At the center of the vapor cell, the signal and controlling beams have $1/e^2$ diameters of 3.8 mm and 4.2 mm, respectively. The cell is mounted inside a 150 mm long solenoid. The guiding magnetic fields are generated by applying currents provided by a stable source to the solenoid. To reduce the environment magnetic field, we place the solenoid into a magnetically shielded cylinder. The length and clear aperture of the magnetically shielded cylinder are ~152 mm and ~9 mm. We use a Lakeshore-421 gauss meter to measure the resident magnetic fields in the solenoid. When the current is not applied to the solenoid, the measured magnetic fields along x-, y- and z-directions are all less than ~10 mG near its two ends, while in the middle (where cell will be placed), the measured magnetic fields are less than 4 mG. With and without the currents being applied, the measured average gradients of magnetic field along z-direction are about ~0.01 mG mm^{-1}.

We demonstrate EIT-based light storages in the Rb vapor cell for different solenoid currents I_0, which can generate different strengths of the guiding field B_{z0}. The input peak powers of the signal and controlling beams are ~15 μW and ~170 mW, respectively. In each experimental circle, we first switch on the V-polarized controlling beam and then send an H-polarized signal pulse with a length of 500 ns to the atomic ensemble. At the falling edge of the signal pulse, we switch off the controlling beam over a short time interval (~50 ns) and then the signal pulse is mapped onto spin waves in the atomic ensemble at the initial time $t_0 = 0$. After a time delay t, we switch on the controlling beam to map the spin waves into the retrieval optical signal. Using another Glan laser polarizer (GLP2), we separate the H-polarized retrieval signal from the V-polarized controlling beam. The H-polarized retrieval signal is direct into a photodetector PD and recorded by it, while, the V-polarized controlling beam is reflected by GLP2.

The measured retrieval efficiencies as a function of storage time t are shown in figure 3. The black square dots in figure 3(a) is measured results for solenoid current $I_0=0$ (corresponding to $B_{z0}=0$), it exhibits a monotonic decreasing with time and a $1/e$ storage time of ~6.2 μs. When solenoid currents are applied to generate the guiding fields, we observe retrieval efficiencies versus storage time t and find obvious increases in coherence times. The black square dots in figures 3(b)–(d) are the measured retrieval efficiencies versus the time t for solenoid currents $I_0=2.09$ mA, 3.06 mA, 5.10 mA. The blue dashed lines in figures 3(b)–(d) are envelopes of the measured retrieval efficiencies, which show

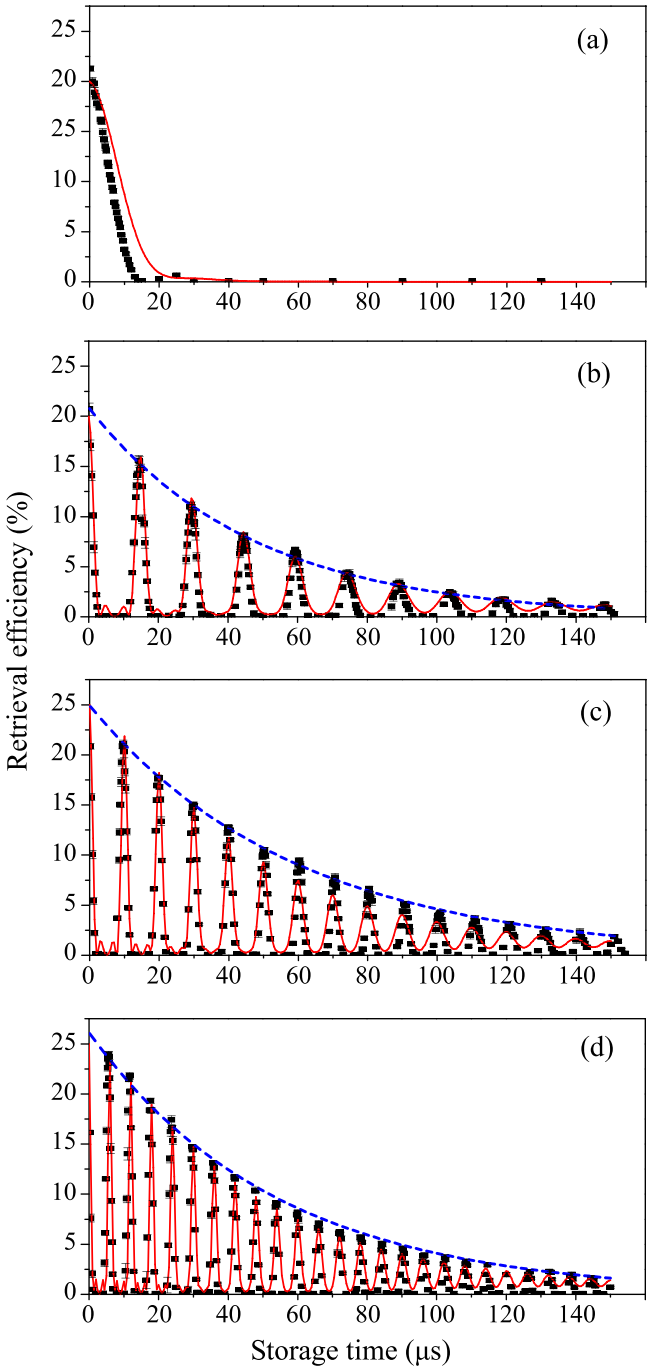

Figure 3. Retrieval efficiencies for different guiding magnetic fields which are generated by varying solenoid currents. The black square dots in figures 3(a)–(d) are the measured retrieval efficiencies versus storage time t for solenoid currents $I_0 = 0$ mA, 2.06 mA, 3.09 mA and 5.10 mA, respectively. The red solid curves are the fittings to the experimental data according to equations (50) and (51) together with equations (4), (13), (37) and (45), which yield the best-fit values of guiding magnetic field $B_{z0} = 0$ mG for (a), $B_{z0} = 63$ mG for (b), $B_{z0} = 93$ mG for (c), $B_{z0} = 169$ mG for (d). The $1/e$ storage time in figure 3(a) is 6.2 μs. The blue dashed lines in figures 3(b)–(d) are envelopes of exponential decays, yielding the lifetimes of 46.1 μs for figures 3(b), 59.1 μs for figure 3(c), 54 μs for figure 3(d), respectively.

$1/e$ storage times of ~46 μs for figure 3(b), ~59 μs for figure 3(c), ~54 μs for figure 3(d), respectively. The retrieval efficiencies versus storage time undergo collapses and revivals when the guiding magnetic fields are applied. Such oscillation behaviors have been observed in cold atoms and are attributed to the interferences between Zeeman coherences [31, 32, 34]. By repeatedly inversing the direction of the guiding magnetic fields during storages or applying a π-pulse sequence [35] on the atoms to swap their population in two ground levels $F = 2$ and $F = 3$, we can expect to remove the oscillation behaviors. The storage lifetimes without the guiding fields (figure 3(a)) are obviously less than that with the guiding fields (figures 3(b)–(d)), the physical reason for this are discussed in detail in the following section.

Table 1. The calculated lifetimes $\tau^{\mathrm{I}}_{m_a,m_b}$ for a spatial gradient of the magnetic field $B'_z = 0.008\ \mathrm{mG\ mm^{-1}}$.

$\tau^{\mathrm{I}}_{2,2}$	$\tau^{\mathrm{I}}_{2,0}$	$\tau^{\mathrm{I}}_{1,3}$	$\tau^{\mathrm{I}}_{1,-1}$	$\tau^{\mathrm{I}}_{1,1}$	$\tau^{\mathrm{I}}_{0,2}$
142 μs	284 μs	142 μs	1.8 s	284 μs	284 μs
$\tau^{\mathrm{I}}_{0,-2}$	$\tau^{\mathrm{I}}_{-1,1}$	$\tau^{\mathrm{I}}_{-1,-1}$	$\tau^{\mathrm{I}}_{-1,-3}$	$\tau^{\mathrm{I}}_{-2,0}$	$\tau^{\mathrm{I}}_{-2,-2}$
284 μs	1.8 s	284 μs	142 μs	284 μs	142 μs

4. Theoretical model for decoherence of spin waves and the fittings to the experimental data

Many processes may cause the decoherence of spin waves in atomic ensembles. We divide the main factors into four classes and discuss them in the following.

(1) Atomic motions. This effect will lead to the drift of atoms in and out of the light beams and then cause decoherence [4]. Considering the decoherence induced by this effect, the spin wave evolves according to

$$\rho_{m_a,m_b}(z,\,t) = \rho_{m_a,m_b}(z,\,t_0)\mathrm{e}^{-t/\tau_d}\mathrm{e}^{-\mathrm{i}\omega^{Bz}_{m_a,m_b}t}, \tag{11}$$

where τ_d is the lifetime limited by this decoherence. τ_d is independent of the magnetic quantum number, it is the same for each spin wave $\rho_{m_a,m_b}(z,\,t)$.

(2) Inhomogeneous Zeeman broadening induced by spatial variations of the magnetic field B_z [34, 36]. Such phenomenon leads to the decoherence of the spin wave $\rho_{m_a,m_b}(z,\,t)$ and make the spin wave evolve according to

$$\rho_{m_a,m_b}(z,\,t) = \rho_{m_a,m_b}(z,\,t_0)\mathrm{e}^{-t/2\tau^{\mathrm{I}}_{m_a,m_b}}\mathrm{e}^{-\mathrm{i}\omega^{Bz}_{m_a,m_b}t}, \tag{12}$$

where, the lifetime limited by this decoherence is [31]

$$\tau^{\mathrm{I}}_{m_a,m_b} = \hbar/\left(\left|g_{Fa}(m_a + m_b) - \delta g m_b\right|\mu_B B'_z l\right) \tag{13}$$

here, B'_z is the spatial gradient of the magnetic field B_z. Assuming that $B'_z = 0.008\ \mathrm{mG\ mm^{-1}}$ which will be used in the fittings in figure 3, we calculated the values of $\tau^{\mathrm{I}}_{m_a,m_b}$ and the results are shown in table 1.

(3) Incoherent population transitions between Zeeman sublevels caused by transverse magnetic field fluctuations $\delta\vec{B}_x(t)$ and $\delta\vec{B}_y(t)$. Such decoherence process has been pointed out by [37], but has not been theoretically

explained in detail until now. In the following, we develop a theoretical model to evaluate the decay of spin waves caused by transverse magnetic field fluctuations $\delta\vec{B}_x(t)$ and/or $\delta\vec{B}_y(t)$.

The time-dependent Schrödinger equation is:

$$i\hbar\frac{\partial\Phi}{\partial t} = \hat{H}\Phi. \tag{14}$$

The Hamiltonian $\hat{H}$ is given by the interaction of the magnetic field $\vec{B}$ with atomic magnetic dipole moment $\vec{\mu}$ and can be written as:

$$\hat{H} = -\hat{\vec{\mu}}\cdot\vec{B} = \frac{g_F\mu_B\hat{\vec{F}}\cdot\vec{B}}{\hbar}, \tag{15}$$

where $\mu_B = 2\pi\cdot\hbar\cdot 1.4\ \mathrm{MHz\,G^{-1}}$ is Bohr magneton, $\vec{B} = B_x\vec{e}_x + B_y\vec{e}_y + B_z\vec{e}_z$ is the magnetic field, here, $B_i = B_{i0} + \delta B_i(t)$ is the magnetic field along i-direction ($i = x$, y, z) (B_{i0} is the bias value and $\delta B_i(t)$ is the fluctuation), $g_F = -g_{F_a} = g_{F_b}$ is Landé g-factor for the $|a\rangle$ or $|b\rangle$ state (where the difference $\delta g = g_{F_a} + g_{F_b}$ is neglected since it is very small), $\hat{\vec{F}} = \hat{F}_x\vec{e}_x + \hat{F}_y\vec{e}_y + \hat{F}_z\vec{e}_z$ is the operator of the hyperfine angular momentum. In the presented experimental system, we set $B_{x0} = B_{y0} = 0$ and $B_{z0} \neq 0$. In the eigenbasis of Zeeman sublevels $\left|a, m_a\right\rangle_z$ $\left(m_a = -2, -1, \ldots +2\right)$, the Hamiltonian $\hat{H}$ can be represented as:

$$\hat{H}^{(a)} = \frac{g_F\mu_B}{2}\begin{bmatrix} 4B_z & 2\delta B_-(t) & 0 & 0 & 0 \\ 2\delta B_+(t) & 2B_z & \sqrt{6}\,\delta B_-(t) & 0 & 0 \\ 0 & \sqrt{6}\,\delta B_+(t) & 0 & \sqrt{6}\,\delta B_-(t) & 0 \\ 0 & 0 & \sqrt{6}\,\delta B_+(t) & -2B_z & 2\delta B_-(t) \\ 0 & 0 & 0 & 2\delta B_+(t) & -4B_z \end{bmatrix} \tag{16}$$

respectively, while, in the eigenbasis $\left|b, m_b\right\rangle_z$ $\left(m_b = -3, -2, \ldots +3\right)$, they can be represented as:

$$\hat{H}^{(b)}(t) = \frac{g_F\mu_B}{2}\begin{bmatrix} 6B_z & \sqrt{6}\,\delta B_-(t) & 0 & 0 & 0 & 0 & 0 \\ \sqrt{6}\,\delta B_+(t) & 4B_z & \sqrt{10}\,\delta B_-(t) & 0 & 0 & 0 & 0 \\ 0 & \sqrt{10}\,\delta B_+(t) & 2B_z & \sqrt{12}\,\delta B_-(t) & 0 & 0 & 0 \\ 0 & 0 & \sqrt{12}\,\delta B_+(t) & 0 & \sqrt{12}\,\delta B_-(t) & 0 & 0 \\ 0 & 0 & 0 & \sqrt{12}\,\delta B_+(t) & -2B_z & \sqrt{10}\,\delta B_-(t) & 0 \\ 0 & 0 & 0 & 0 & \sqrt{10}\,\delta B_+(t) & -4B_z & \sqrt{6}\,\delta B_-(t) \\ 0 & 0 & 0 & 0 & 0 & \sqrt{6}\,\delta B_+(t) & -6B_z \end{bmatrix} \tag{17}$$

respectively, where, $\delta B_\pm(t) = \delta B_x(t) \pm i\delta B_y(t)$ denote the transverse field noise. The wavefunctions in the $F = 2$ and $F = 3$ subspaces can be written as

$$\Phi_{F_a} = \sum_{m_a=-2}^{2} c_{m_a}(t)e^{-im_a\omega_L t}\left|a, m_a\right\rangle \tag{18a}$$

and

$$\Phi_{F_b} = \sum_{m_b=-3}^{3} c_{m_b}(t)e^{-im_b\omega_L t}\left|b, m_b\right\rangle \tag{18b}$$

respectively, where $\omega_L = \omega_{L0} + \delta\omega_L$ with $\omega_{L0} = g_F\mu_B B_{z0}/\hbar$ and $\delta\omega_L = g_F\mu_B\delta B_z/\hbar$ being the Larmor frequency induced by the magnetic field B_{z0} and the magnetic field fluctuation δB_z, respectively. Substituting equation (18) into the time-dependent Schrödinger equation (14), we obtain

$$\begin{aligned} i\hbar\frac{\partial C_{m_a}}{\partial t} = \frac{g_F\mu_B}{2}\Big[&\sqrt{(F-m_a)(F+m_a+1)}\,\delta B_+(t) \\ &\times C_{m_a+1}e^{-i\omega_L t} + \sqrt{(F+m_a)(F-m_a+1)} \\ &\times \delta B_-(t)C_{m_a-1}e^{i\omega_L t}\Big] \end{aligned} \tag{19a}$$

and

$$\begin{aligned} i\hbar\frac{\partial C_{m_b}}{\partial t} = \frac{g_F\mu_B}{2}\Big[&\sqrt{(F-m_b)(F+m_b+1)}\,\delta B_+(t) \\ &\times C_{m_b+1}e^{-i\omega_L t} + \sqrt{(F+m_b)(F-m_b+1)} \\ &\times \delta B_-(t)C_{m_b-1}e^{i\omega_L t}\Big] \end{aligned} \tag{19b}$$

respectively. In the above equations, we have assumed $\partial(\delta B_z)/\partial t \to 0$ since the varying of δB_z is very small during each experimental measurement. The transverse field noises include $\delta B_x(t)$ and $\delta B_y(t)$ components, which may be written as $\delta B_x(t) = \int_{-\infty}^{\infty}\delta B_x(\omega_x)\cos\omega_x t\,d\omega_x$ and $\delta B_y(t) = \int_{-\infty}^{\infty}\delta B_y(\omega_y)\cos\omega_y t\,d\omega_y$, respectively, where $\omega_{x,y}$ are the frequencies of noisy magnetic fields. According to equation (19), we may see that the magnetic field noises $\delta B_x(t)$ and/or $\delta B_y(t)$ will cause atomic transitions between Zeeman sublevels. Before the optical storage, the atoms are prepared in every Zeeman sublevel $\left|b, m_b\right\rangle$ with equal probability. At the time $t = t_0 = 0$, the optical signal is stored, a small number of the atoms are transferred from the state $\left|b, m_b\right\rangle$ into the state $\left|a, m_a\right\rangle$ $\left(m_a = m_b - 1, m_b, m_b + 1\right)$.

If the atom is in the state $\left|a, m_a\right\rangle$ at the initial time $t = 0$, the first-order approximation allow us to only consider the transitions from $\left|a, m_a\right\rangle$ state to $\left|a, m_a \pm 1\right\rangle$ states. Thus, the

equation (19*a*) can be rewrited as

$$\mathrm{i}\hbar\frac{\partial C_{m_a+1}(t)}{\partial t} = G^{+}_{m_a}\Big(\int_{-\infty}^{\infty}\big(\delta B_x(\omega_x)\cos\omega_x t\big)\mathrm{d}\omega_x - \mathrm{i}\int_{-\infty}^{\infty}\big(\delta B_y(\omega_y)\cos\omega_y t\big) \times \mathrm{d}\omega_y\Big)C_{m_a}(t)\mathrm{e}^{\mathrm{i}\omega_L t}, \tag{20a}$$

$$\mathrm{i}\hbar\frac{\partial C_{m_a-1}(t)}{\partial t} = G^{-}_{m_a}\Big(\int_{-\infty}^{\infty}\big(\delta B_x(\omega_x)\cos\omega_x t\big)\mathrm{d}\omega_x + \mathrm{i}\int_{-\infty}^{\infty}\big(\delta B_y(\omega_y)\cos\omega_y t\big) \times \mathrm{d}\omega_y\Big)C_{m_a}(t)\mathrm{e}^{-\mathrm{i}\omega_L t}, \tag{20b}$$

where, $G^{-}_{m_a} = \frac{g_F\mu_B}{2\hbar}\sqrt{(F_a+m_a)(F_a-m_a+1)}$ and $G^{+}_{m_a} = \frac{g_F\mu_B}{2\hbar}\sqrt{(F_a-m_a)(F_a+m_a+1)}$. Integrations of the equations (20*a*) and (20*b*) over time t give the first-order approximations, which are

$$C_{m_a\pm1}(t) \simeq \left(\int_{-\infty}^{\infty} G^{\pm}_{m_a}\delta B_x(\omega_x)\mathrm{e}^{\mathrm{i}\frac{\Delta\omega_x t}{2}}\frac{\sin\frac{\Delta\omega_x t}{2}}{\Delta\omega_x}\mathrm{d}\omega_x \mp \mathrm{i}\int_{-\infty}^{\infty} G^{\pm}_{m_a}\delta B_y(\omega_y)\mathrm{e}^{\mathrm{i}\frac{\Delta\omega_y t}{2}}\frac{\sin\frac{\Delta\omega_y t}{2}}{\Delta\omega_y}\mathrm{d}\omega_y\right) \tag{21}$$

where, $\Delta\omega_{x(y)} = \omega_{x(y)} - \omega_L$. So, at time t, the probabilities of atom transferred from the state $|a, m_a\rangle$ into the states $|a, m_a \pm 1\rangle$ are $\left|C_{m_a\pm1}(t)\right|^2$. Such population transfers are incoherent, the reason is that the coherences $\left\langle\rho_{m_a\pm1,m_a}\right\rangle = \left\langle C_{m_a\pm1}(t)C_{m_a}(t)\right\rangle \propto 0$, where $\langle\ldots\rangle$ denotes the average over the distribution of the magnetic field δB_x or δB_y, and $\left\langle\delta B_x(\omega_x)\right\rangle = \left\langle\delta B_y(\omega_y)\right\rangle = 0$ is used. The incoherent population transfers will induce decoherence of the spin wave $\rho_{m_a,m_b}(z,\ t)$ and limit its storage lifetime. We now calculate the lifetimes for the two following case.

(i) The lifetime for the guiding field $B_{z0}=0$. For $B_{z0}=0$, the Larmor precession frequency $\omega_L = g_F\mu_B\left(B_{z0}+\delta B_z\right)/\hbar \to 0$ due to that the magnetic-field noise δB_z is very small and can be neglected. In this case, the probability amplitudes $C_{m_a\pm1}(t)$ in equation (21) can be expressed as:

$$C_{m_a\pm1}(t) \simeq \left(\int_{-\infty}^{\infty} G^{\pm}_{m_a}\delta B_x(\omega_x)\mathrm{e}^{\mathrm{i}\frac{\omega_x t}{2}}\frac{\sin\frac{\omega_x t}{2}}{\omega_x}\mathrm{d}\omega_x \mp \mathrm{i}\int_{-\infty}^{\infty} G^{\pm}_{m_a}\delta B_y(\omega_y)\mathrm{e}^{\mathrm{i}\frac{\omega_y t}{2}}\frac{\sin\frac{\omega_y t}{2}}{\omega_y}\mathrm{d}\omega_y\right). \tag{22}$$

Averaging over the distributions of magnetic field noises δB_x or δB_y, we calculate the average transition probabilities $\left\langle\left|C_{m_a\pm1}(t)\right|^2\right\rangle$, which are

$$\begin{aligned}\left\langle\left|C_{m_a\pm1}(t)\right|^2\right\rangle &= \int_{-\infty}^{\infty}\int_{-\infty}^{\infty}\left|G^{\pm}_{m_a}\right|^2\left\langle\delta B_x(\omega_x)\delta B_x\left(\omega_x{}'\right)\right\rangle \\ &\times \mathrm{e}^{\mathrm{i}\frac{(\omega_x-\omega_x{}')t}{2}}\frac{\sin\frac{\omega_x t}{2}}{\omega_x}\frac{\sin\frac{\omega_x{}' t}{2}}{\omega_x{}'}\mathrm{d}\omega_x\mathrm{d}\omega_x{}' \\ &+ \int_{-\infty}^{\infty}\int_{-\infty}^{\infty}\left|G^{\pm}_{m_a}\right|^2\left\langle\delta B_y(\omega_y)\delta B_y\left(\omega_y{}'\right)\right\rangle \\ &\times \mathrm{e}^{\mathrm{i}\frac{(\omega_y-\omega_y{}')t}{2}}\frac{\sin\frac{\omega_y t}{2}}{\omega_y}\frac{\sin\frac{\omega_y{}' t}{2}}{\omega_y{}'}\mathrm{d}\omega_y\mathrm{d}\omega_y{}'.\end{aligned} \tag{23}$$

The frequency correlation for a stationary process can be written as

$$\left\langle\delta B_x(\omega_x)\cdot\delta B_x\left(\omega_x{}'\right)\right\rangle = S(\omega_x)\delta\left(\omega_x-\omega_x{}'\right), \tag{24a}$$

$$\left\langle\delta B_y(\omega_y)\cdot\delta B_y\left(\omega_y{}'\right)\right\rangle = S(\omega_y)\delta\left(\omega_y-\omega_y{}'\right), \tag{24b}$$

where, $S(\omega_x) = \left\langle\delta B_x(\omega)\cdot\delta B_x(\omega)\right\rangle$ and $S(\omega_y) = \langle\delta B_y(\omega_y)\cdot\delta B_y(\omega_y)\rangle$ are the noise power spectrums. Substituting equation (24) into equation (23), we obtain:

$$\left\langle\left|C_{m_a\pm1}(t)\right|^2\right\rangle = \frac{\left|G^{\pm}_{m_a}\right|^2}{4}t^2\left(\int_{-\infty}^{\infty}S(\omega_x)\frac{\sin^2\left(\omega_x t/2\right)}{\left(t\omega_x/2\right)^2}\mathrm{d}\omega_x + \int_{-\infty}^{\infty}S(\omega_y)\frac{\sin^2\left(\omega_y t/2\right)}{\left(t\omega_y/2\right)^2}\mathrm{d}\omega_y\right). \tag{25}$$

We assume that the noise spectrum $S(\omega_x)$ and $S(\omega_y)$ in the presented system are strong at low frequencies and small at high frequencies. Such noise spectrums are agreement with the feature of typical 1/*f* noise [38], and observed in optically trapped atom system [39]. So, $S(\omega_{x(y)})$ will be close to zero when its frequency goes beyond a enough large range of $[-\Delta\omega, \Delta\omega]$. In this case, the integration range in the equation (25) can be changed from $[-\infty, \infty]$ into $[-\Delta\omega, \Delta\omega]$. Moreover, if the time t is short enough to make $\Delta\omega t \ll 1$, we have $\frac{\sin^2(\omega_x t/2)}{(\omega_x t/2)^2} \to 1$ and $\frac{\sin^2\left(\omega_y t/2\right)}{\left(\omega_y t/2\right)^2} \to 1$ for $-\Delta\omega < \omega_{x(y)} < \Delta\omega$.

Thus, the probabilities of finding an atom in the states $|a, m_a \pm 1\rangle$ are:

$$\left\langle\left|C_{m_a\pm1}(t)\right|^2\right\rangle = \frac{\left|G^{\pm}_{m_a}\right|^2 t^2}{4}\left(\int_{-\Delta\omega}^{\Delta\omega}S(\omega_x)\mathrm{d}\omega_x + \int_{-\Delta\omega}^{\Delta\omega}S(\omega_y)\mathrm{d}\omega_y\right) = \left|G^{\pm}_{m_a}\right|^2 t^2 P/2, \tag{26}$$

where $P = \int_{-\Delta\omega}^{\Delta\omega}S(\omega_x)\mathrm{d}\omega_x = \int_{-\Delta\omega}^{\Delta\omega}S(\omega_y)\mathrm{d}\omega_y$ is the noise power of the magnetic field δB_x or δB_y, it also can be

expressed as

$$P = \left\langle \left|\delta B_x(t)\right|^2 \right\rangle = \left\langle \left|\delta B_y(t)\right|^2 \right\rangle. \tag{27}$$

As pointed out above, the population transfers from the state $\left|a, m_a\right\rangle$ to the state $\left|a, m_a \pm 1\right\rangle$ induced by the transverse magnetic fields are incoherent. So, the population transfer rates are:

$$R_{m_a \to m_a \pm 1}(t) = -\frac{\mathrm{d}\left\langle \left|C_{m_a \pm 1}\right|^2 \right\rangle}{\mathrm{d}t} \simeq -\frac{\left|G^{\pm}_{m_a}\right|^2 tP}{2}. \tag{28}$$

The rate equation for the population transfer from the state $\left|a, m_a\right\rangle$ to $\left|a, m_a \pm 1\right\rangle$ is

$$\frac{\mathrm{d}N_{m_a}(t)}{\mathrm{d}t} = \left(R_{m_a \to m_a+1}(t) + R_{m_a \to m_a-1}(t)\right)N_{m_a}(t). \tag{29}$$

Thus, we can obtain the time-dependence population decay for the state $\left|a, m_a\right\rangle$, which is

$$N_{m_a}(t) = N_{m_a}(0)\mathrm{e}^{-\frac{t^2}{\tau^2_{m_a}}} \tag{30}$$

where,

$$\tau_{m_a} = \sqrt{\frac{4}{\left(\left|G^{+}_{m_a}\right|^2 + \left|G^{-}_{m_a}\right|^2\right)P}}, \tag{31}$$

$N_{m_a}(0) = Np\ \left(p = 1/(2F_a + 1)\right)$ is the initial population of the state $\left|a, m_a\right\rangle$.

If an atom is in the state $\left|b, m_b\right\rangle$ at the time $t = t_1$, it will decay with time due to equation (30). Similar to the calculation of $N_{m_a}(t)$, we obtain the time-dependence population in the state $\left|b, m_b\right\rangle$ according to equation (19*b*), which is

$$N_{m_b}(t) = N_{m_b}(0)\mathrm{e}^{-\frac{t^2}{\tau^2_{m_b}}}, \tag{32}$$

where,

$$\tau_{m_b} = \sqrt{\frac{4}{\left(\left|G^{+}_{m_b}\right|^2 + \left|G^{-}_{m_b}\right|^2\right)P}}. \tag{33}$$

With

$$\left|G^{\pm}_{m_b}\right| = \mu_B \left|g_F\right| \sqrt{\left(F_b \mp m_b\right)\left(F_b \pm m_b + 1\right)}/(2\hbar). \tag{34}$$

The excitation number of spin wave $\rho_{m_a,m_b}(z, t)$ is defined as:

$$N^e_{m_a,m_b}(t) = Np\left\langle \left(\rho_{m_a,m_b}(z, t)\right)^{\dagger}\rho_{m_a,m_b}(z, t) \right\rangle. \tag{35}$$

According to this definition, we have

$$\begin{aligned} N^e_{m_a,m_b}(t) &= Np\left\langle \left|C_{m_a}(t)\right|^2 \left|C_{m_b}(t)\right|^2 \right\rangle \\ &= Np\left\langle \left|C_{m_a}(t)\right|^2 \right\rangle \left\langle \left|C_{m_b}(t)\right|^2 \right\rangle \\ &= N_{m_a}(0)\mathrm{e}^{-\frac{t^2}{\tau^2_{m_a}}}\left\langle \left|C_{m_b}(t)\right|^2 \right\rangle \\ &= N_{m_b}(0)\mathrm{e}^{-t^2\left(\frac{1}{\tau^2_{m_b}}+\frac{1}{\tau^2_{m_a}}\right)} \\ &= N^e_{m_a,m_b}(0)\mathrm{e}^{-\left(\frac{t}{\tau^{\mathrm{II}}_{m_a,m_b}}\right)^2}, \end{aligned} \tag{36}$$

where, $N^e_{m_a,m_b}(0)$ is the initial excitation number of the spin wave $\rho_{m_a,m_b}(z, t)$, which equals to $N_{m_b}(0)$,

$$\tau^{\mathrm{II}}_{m_a,m_b} = \frac{\tau_{m_a}\tau_{m_b}}{\sqrt{\tau^2_{m_a} + \tau^2_{m_b}}}. \tag{37}$$

According to the equations (35) and (36), we may obtain the time-dependent $\left\langle \rho_{m_a,m_b}(z, t) \right\rangle$, which is:

$$\left\langle \rho_{m_a,m_b}(z, t) \right\rangle = \rho_{m_a,m_b}(z, t_0)\mathrm{e}^{-t^2/2\left(\tau^{\mathrm{II}}_{m_a,m_b}\right)^2} \tag{38}$$

For the presented experimental setup, the evaluated average fluctuations of magnetic fields are $\sqrt{\left\langle \left|\delta B_x\right|^2 \right\rangle} \approx \sqrt{\left\langle \left|\delta B_y\right|^2 \right\rangle} \approx 5$ mG. Substituting these data into the equation (27) to obtain the noise power P, we can calculate τ_{m_a} and τ_{m_b} based on equations (31) and (33), respectively, and then we can calculate $\tau^{\mathrm{II}}_{m_a,m_b}$ based on equation (37). The calculated lifetimes for different Zeeman coherences are shown in table 2, the results show that the lifetimes are in the range from ~32 μs to ~48 μs.

(ii) The lifetime for a large enough guiding field B_{z0}. Assuming that the atom is initially prepared in the state $\left|a, m_a\right\rangle$ and neglecting the Larmor frequency induced by δB_z, we may write the probability amplitudes $C_{m_a \pm 1}(t)$ at time t as:

$$\begin{aligned} \left\langle \left|C_{m_a \pm 1}(t)\right|^2 \right\rangle = \frac{\left|G^{\pm}_{m_a}\right|^2}{4}t^2\Bigg(&\int_{-\infty}^{\infty} S(\omega_x) \\ &\times \frac{\sin^2\frac{(\omega_x - \omega_{L_0})t}{2}}{\left(\frac{(\omega_x - \omega_{L_0})t}{2}\right)^2}\mathrm{d}\omega_x + \int_{-\infty}^{\infty} S(\omega_y) \\ &\times \frac{\sin^2\frac{(\omega_y - \omega_{L_0})t}{2}}{\left(\frac{(\omega_y - \omega_{L_0})t}{2}\right)^2}\mathrm{d}\omega_y \Bigg). \end{aligned} \tag{39}$$

If the guiding field B_{z0} is enough strong to make $B_{z0} \gg \frac{\hbar\Delta\omega_{x,y}}{2g_F\mu_B}$

Table 2. The calculated lifetimes $\tau^{\mathrm{II}}_{m_a,m_b}$ for the case of $B_{z0}=0$ and $\sqrt{\left\langle \left|\delta B_x\right|^2 \right\rangle} \approx \sqrt{\left\langle \left|\delta B_y\right|^2 \right\rangle} \approx 5$ mG.

$\tau^{\mathrm{II}}_{2,2}$	$\tau^{\mathrm{II}}_{2,0}$	$\tau^{\mathrm{II}}_{1,3}$	$\tau^{\mathrm{II}}_{1,-1}$	$\tau^{\mathrm{II}}_{1,1}$	$\tau^{\mathrm{II}}_{0,2}$	$\tau^{\mathrm{II}}_{0,0}$
43.0 μs	36.2 μs	48.2 μs	34.0 μs	34.0 μs	36.2 μs	32.1 μs
$\tau^{\mathrm{II}}_{0,-2}$	$\tau^{\mathrm{II}}_{-1,1}$	$\tau^{\mathrm{II}}_{-1,-1}$	$\tau^{\mathrm{II}}_{-1,-3}$	$\tau^{\mathrm{II}}_{-2,0}$	$\tau^{\mathrm{II}}_{-2,-2}$	—
36.2 μs	34.0 μs	34.0 μs	48.2 μs	36.2 μs	43.0 μs	—

(i.e., $\omega_{L_0} \gg \Delta\omega_{x,y}/2$, where $\Delta\omega_{x,y}$ is full width at half maximum of the noise power spectrum $S(\omega_{x,y})$), the degeneracy of Zeeman sublevels will be obviously lifted and the dominant components of the magnetic fields noise $\delta B_{x,y}$ will be far off-resonance with the transitions between Zeeman sublevels $\left|a, m_a\right\rangle$ and $\left|a, m_a \pm 1\right\rangle$. In this case, after a long time t, the transition probabilities between Zeeman sublevels will be very small and the first-order approximation in equation (39) is still applicable to calculating $\left|C_{m_a\pm1}(t)\right|^2$. For the long time t, the identity $\lim_{a\to\infty}\left(\frac{\sin^2 a(x-x_0)}{\pi a(x-x_0)^2}\right) \to \delta(x-x_0)$, implies that

$$\left\langle \left|C_{m_a\pm1}(t)\right|^2 \right\rangle = \frac{\left|G^{\pm}_{m_a}\right|^2}{4}\pi S(\omega_{L_0})t. \tag{40}$$

So, the population transfer rates are:

$$R_{m_a\to m_a\pm1}(t) = -\frac{\mathrm{d}\left\langle \left|C_{m_a\pm1}\right|^2 \right\rangle}{\mathrm{d}t} \simeq -\frac{\left|G^{\pm}_{m_a}\right|^2 \pi S(\omega_{L_0})}{2}. \tag{41}$$

According to the above expression, we obtain the time-dependence population decay for the state $\left|a, m_a\right\rangle$, which is

$$N_{m_a}(t) = N_{m_a}(0)\mathrm{e}^{-\frac{t}{\tau^{\mathrm{II}}_{m_a}}} \tag{42}$$

where,

$$\tau^{\mathrm{II}}_{m_a} = \frac{2}{\left(\left|G^{+}_{m_a}\right|^2 + \left|G^{-}_{m_a}\right|^2\right)\pi S(\omega_{L_0})}. \tag{43}$$

Similar to the calculation of $N_{m_a}(t)$, we can calculate $N_{m_b}(t)$ if the atoms are initially prepared in the state $\left|b, m_b\right\rangle$ (i.e., $N_{m_b}(0) = 1$), which is

$$N_{m_b}(t) = N_{m_b}(0)\mathrm{e}^{-\frac{t}{\tau^{\mathrm{II}}_{m_b}}} \tag{44}$$

where,

$$\tau^{\mathrm{II}}_{m_b} = \frac{2}{\left(\left|G^{+}_{m_b}\right|^2 + \left|G^{-}_{m_b}\right|^2\right)\pi S(\omega_{L_0})}. \tag{45}$$

For the enough strong applied guiding magnetic field B_{z0}, ω_{L_0} will be very large and thus $S\left(\omega_{L_0}\right)$ will be close to zero. In this case, $\tau^{\mathrm{II}}_{m_a(m_b)} \to \infty$, which means that decoherence caused by the magnetic field noises can be suppressed.

(4) Dephasing induced by the fluctuation $\delta B_z(t)$. The magnetic field fluctuation δB_z will cause a Larmor precession with a frequency $\delta\omega_L = \mu_B \delta B_z g_F/\hbar$ and then the SW ρ_{m_a,m_b} will acquire a random phase $\varphi^{\delta B_z}_{m_a,m_b} = \delta\omega_L(m_a + m_b)t$. This random phase will induce a degradation of the retrieval efficiency with time. We explain such degradation based on the expression of the retrieval efficiency $\eta_H(t)$ (equation (10)). In the expanding expression, the terms

$$\begin{aligned} C_{m_a,m_b,m'_a,m'_b} &\propto \exp\left(-\mathrm{i}\left(\omega^{B_{z0}}_{m_a,m_b} + \omega^{\delta B_z}_{m_a,m_b}\right)\right. \\ &\left. + \mathrm{i}\left(\omega^{B_{z0}}_{m_a',m_b'} + \omega^{\delta B_z}_{m_a',m_b'}\right)\right)t \\ &= \exp\left[-\mathrm{i}\left(\omega^{B_{z0}}_{m_a,m_b} - \omega^{B_{z0}}_{m_a',m_b'}\right)t\right] \\ &\times\left[\mathrm{i}\frac{\mu_B g_{F_a}}{\hbar}\left(m'_a + m'_b - m_a - m_b\right)\delta B_z t\right], \end{aligned} \tag{46}$$

(where $m_a \neq m'_a$ or $m'_b \neq m_b$) involve in a random phase induced by δB_z. Averaging over the distribution of δB_z gives:

$$\begin{aligned} \left\langle C_{m_a,m_b,m'_a,m'_b}\right\rangle &\propto \exp\left[-\mathrm{i}\left(\omega^{B_{z0}}_{m_a,m_b} - \omega^{B_{z0}}_{m_a',m_b'}\right)t\right] \\ &\times\int \mathrm{d}\left(\delta B_z\right)p\left(\delta B_z\right)\exp\left[\mathrm{i}\frac{\mu_B g_{F_a}}{\hbar}\left(m'_a\right.\right. \\ &\left.\left. + m'_b - m_a - m_b\right)\delta B_z t\right]. \end{aligned} \tag{47}$$

We now assume that the magnetic field δB_z is a Gaussian distribution, i.e.,

$$p\left(\delta B_z\right) = \frac{1}{\sqrt{\pi}\Delta B_z}\exp\left(-\frac{\delta {B_z}^2}{\Delta {B_z}^2}\right). \tag{48}$$

Where $\Delta B_z = \sqrt{2}\sqrt{\left\langle \left|\delta B_z\right|^2 \right\rangle}$ is the width of the field distribution, $\sqrt{\left\langle \left|\delta B_z(t)\right|^2 \right\rangle}$ is the average fluctuation of magnetic field along z-direction. In this case, the average terms $\left\langle C_{m_a,m_b,m'_a,m'_b}\right\rangle$ becomes

$$\begin{aligned} \left\langle C_{m_a,m_b,m'_a,m'_b}\right\rangle &\propto \exp\left[-\mathrm{i}\left(\omega^{B_{z0}}_{m_a,m_b} - \omega^{B_{z0}}_{m_a',m_b'}\right)t\right] \\ &\times\exp\left(-\left(\frac{\mu_B g_{F_a}}{2\hbar}\left(m'_a + m'_b - m_a - m_b\right)\Delta B_z t\right)^2\right), \end{aligned} \tag{49}$$

which shows a Gaussian decay with time. Due to such decoherence, the retrieval efficiency $\eta_H(t)$ will degrade with time. In the fitting of retrieval efficiency to experimental data,

we take into account such decoherence by averaging over the Gaussian distribution of the magnetic field δB_z. The used formula is

$$\begin{aligned}\left\langle \eta_H(t)\right\rangle = \frac{\eta_H(0)}{4R^4}\int_{-\infty}^{\infty} p\left(\delta B_z\right)\Bigg|\sum_{m_a=-2}^{2}\left|R^{\beta=\alpha}_{m_a,\alpha=1}\right|^2 \\ \times \mathrm{e}^{-f_{ma,mb}(t)-\mathrm{i}\omega^{Bz}_{ma,mb}t} + \sum_{m_a=-1}^{2}\left|R^{\beta=-\alpha}_{m_a,\alpha=1}\right|^2 \\ \times \mathrm{e}^{-f_{ma,mb}(t)-\mathrm{i}\omega^{Bz}_{ma,mb}t} + \sum_{m_a=-2}^{2}\left|R^{\beta=\alpha}_{m_a,\alpha=-1}\right|^2 \\ \times \mathrm{e}^{-f_{ma,mb}(t)-\mathrm{i}\omega^{Bz}_{ma,mb}t} + \sum_{m_a=-2}^{1}\left|R^{\beta=-\alpha}_{m_a,\alpha=-1}\right|^2 \\ \times \mathrm{e}^{-f_{ma,mb}(t)-\mathrm{i}\omega^{Bz}_{ma,mb}t}\Bigg|^2 \mathrm{d}\left(\delta B_z\right). \qquad (50)\end{aligned}$$

According to the above theoretical analysis (1), (2) and (3), we can write:

$$\mathrm{e}^{-f_{ma,mb}(t)} = \mathrm{e}^{-t/2\tau^{1}_{ma,mb}-t^2/2\left(\tau^{\mathrm{II}}_{ma,mb}\right)^2-t/2\tau_d} \qquad (51)$$

Based on equations (50) and (51) together with equations (4), (13) and (37), (45), we give the fittings (the red lines) to the experimental data in figure 3(a) (figures 3(b)–(d)). The best-fit values are $\tau_d = 150\ \mu$s, $B'_z = 0.008$ mG mm^{-1}, $\sqrt{\left\langle\left|\delta B_x(t)\right|^2\right\rangle} = \sqrt{\left\langle\left|\delta B_y(t)\right|^2\right\rangle} = 5$ mG, $\Delta B_z = 3$ mG for figures 3(a)–(d), $B_{z0}=0$ for figure 3(a), $B_{z0} = 63$ mG, $\tau^{\mathrm{II}}_{m_a,m_b}\to\infty$ for figure 3(b), $B_{z0} = 93$ mG, $\tau^{\mathrm{II}}_{m_a,m_b}\to\infty$ for figure 3(c), and $B_{z0} = 169$ mG, $\tau^{\mathrm{II}}_{m_a,m_b}\to\infty$ for figure 3(d). Figure 3(a) shows a quite discrepancy between the experimental data and the model for zero bias field, we attribute the main reason to the imperfect way of modeling the decoherence.

5. Conclusion

In conclusion, we experimentally observed that lifetime of optical storage can be extended from ~6 μs to ~59 μs by applying a guiding magnetic field in a warm atomic vapor. A theory model is developed to evaluate the incoherent population transitions induced by fluctuations of transverse magnetic fields $\delta B_x(t)$ and $\delta B_y(t)$. Based on this evaluation, we explain why lifetimes of light storages can be extended by applying a guiding magnetic field. The developed theory model will help people to understand the fact that the population of atoms prepared in a Zeeman sublevel will fast decay if quantum-axis direction is not fixed. We hope that the measured dependence of the lifetimes on the applied guiding magnetic fields can help people to easily achieve a longer storage lifetime in various memory systems based on warm vapor, for example, room-temperature fiber-integrated optical memory [40], and then find applications in quantum information.

Acknowledgment

We acknowledge funding support from the 973 Program (2010CB923103), the National Natural Science Foundation of China (No. 11475109, 11274211, 60821004).

References

[1] Lvovsky A I, Sanders B C and Tittel W 2009 *Nat. Photonics* **3** 706
[2] Sangouard N, Simon C, Minar J, Binden H Z, de Riedmatten H and Gisin N 2007 *Phys. Rev.* A **76** 050301 (R)
[3] Duan L M, Lukin M D, Cirac J I and Zoller P 2001 *Nature* **414** 413
[4] Pan J W, Chen Z B, Lu C Y, Weinfurter H, Zeilinger A and Żukowski M 2012 *Rev. Mod. Phys.* **84** 777
[5] Fleischhauer M and Lukin M D 2000 *Phys. Rev. Lett.* **84** 5094
[6] Hosseini M, Sparkes B M, Campbell G, Lam P K and Buchler B C 2011 *Nat. Commun.* **2** 174
[7] Nunn J *et al* 2007 *Phys. Rev.* A **75** 011401 (R)
[8] Julsgaard B, Sherson J, Cirac J I, Fiurasek J and Polzik E S 2004 *Nature* **432** 482
[9] de Riedmatten H, Afzelius M, Staudt M U, Simon C and Gisin N 2008 *Nature* **456** 773
[10] Turukhin A V, Sudarshanam V S, Shahriar M S, Musser J A, Ham B S and Hemmer P R 2001 *Phys. Rev. Lett.* **88** 023602
[11] Bigelow M S, Lepeshkin N N and Boyd R W 2003 *Science* **301** 200
[12] Liu C, Dutton Z, Behroozi C H and Hau L V 2001 *Nature* **409** 490
[13] Choi K S, Deng H, Laurat J and Kimble H J 2008 *Nature* **452** 67
[14] Kuzmich A *et al* 2003 *Nature* **423** 731
[15] Phillips D, Fleischhauer A, Mair A, Walsworth R and Lukin M D 2001 *Phys. Rev. Lett.* **86** 783
[16] England D G *et al* 2012 *J. Phys. B: At. Mol. Opt. Phys.* **45** 124008
[17] Reim K F *et al* 2010 *Nat. Photonics* **4** 218
[18] Cho Y-W and Kim Y-H 2010 *Opt. Express* **18** 25786
[19] van der Wal C H *et al* 2003 *Science* **301** 196
[20] Jiang W, Han C, Xue P, Duan L and Guo G-C 2004 *Phys. Rev.* A **69** 043819
[21] Bashkansky M, Fatemi F K and Vurgaftman I 2012 *Opt. Lett.* **37** 142
[22] Hosseini M, Campbell G, Sparkes B M, Lam P K and Buchler B C 2011 *Nat. Phys.* **7** 794–8
[23] Cviklinski J, Ortalo J, Laurat J, Bramati A, Pinard M and Giacobino E 2008 *Phys. Rev. Lett.* **101** 133601
[24] Reim K F, Michelberger P, Lee K C, Nunn J, Langford N K and Walmsley I A 2011 *Phys. Rev. Lett.* **107** 053603
[25] Eisaman M D *et al* 2005 *Nature* **438** 837
[26] Appel J, Figueroa E, Korystov D, Lobino M and Lvovsky A I 2008 *Phys. Rev. Lett.* **100** 093602
[27] Specht H P, Nolleke C, Reiserer A, Uphoff M, Figueroa E, Ritter S and Rempe G 2011 *Nature* **473** 190
[28] Rosenfeld W 2008 Experiments with an entangled system of a single atom and a single photon *PhD Thesis* Maximilians University, Ludwig
[29] Karpa L, Vewinger F and Weitz M 2008 *Phys. Rev. Lett.* **101** 170406

[30] Xu Z, Wu Y, Liu H, Li S and Wang H 2013 *Phys. Rev.* A **88** 013423
[31] Jenkins S D, Matsukevich D N, Chanelière T, Kuzmich A and Kennedy T A B 2006 *Phys. Rev.* A **73** 021803 (R)
[32] Matsukevich D N, Chanelière T, Jenkins S D, Lan S-Y, Kennedy T A B and Kuzmich A 2006 *Phys. Rev. Lett.* **96** 033601
[33] Gorshkov A V, André A, Lukin M D and Sørensen A S 2007 *Phys. Rev.* A **76** 033805
[34] Dudin Y O, Zhao R, Kennedy T A B and Kuzmich A 2010 *Phys. Rev.* A **81** 041805
[35] Kao J T, Hung J T, Chen P and Mou C Y 2010 *Phys. Rev.* A **82** 062120
[36] Zhao R, Dudin Y O, Jenkins S D, Campbell C J, Matsukevich D N, Kennedy T A B and Kuzmich A 2009 *Nat. Phys.* **5** 100
[37] Riedl S, Lettner M, Vo C, Baur S, Rempe G and Dürr S 2012 *Phys. Rev.* A **85** 022318
[38] Paladino E, Galperin Y M, Falci G and Altshuler B L 2014 *Rev. Mod. Phys.* **86** 361
[39] Rosenfeld W, Volz J, Weber M and Weinfurter H 2011 *Phys. Rev.* A **84** 022343
[40] Sprague M R, Michelberger P S, Champion T F M, England D G, Nunn J, Jin X-M, Kolthammer W S, Abdolvand A, Russell P S J and Walmsley I A 2014 *Nat. Phys.* **8** 287–91